

## Ultrastructural morphology and expression of proteoglycans, $\beta$ ig-h3, tenascin-C, fibrillin-1, and fibronectin in bullous keratopathy

Saeed Akhtar, Anthony J Bron, Nicholas R Hawksworth, Richard E Bonshek, Keith M Meek

### Abstract

**Aims**—To investigate the ultrastructural localisation of proteoglycans (PG),  $\beta$ ig-h3 (keratoepithelin), tenascin-C (TN-C), fibrillin, and fibronectin in bullous keratopathy (BK) corneas.

**Methods**—Five corneas from cases of pseudophakic bullous keratopathy (BK) were examined by electron microscopy. PG were demonstrated using cuproinic blue, and the proteins  $\beta$ ig-h3, TN-C, fibrillin, and fibronectin were immunolocalised with rabbit anti- $\beta$ ig-h3, mouse anti-TN-C (BC10 and TN2), mouse anti-fibrillin-1 (MAB2502), mouse anti-fibrillin (MAB1919), and rabbit anti-fibronectin by using a standard immunogold technique.

**Results**—Epithelial cells contained numerous vacuoles. Epithelial folds and large, electron lucent subepithelial bullae were present. Basal lamina was thickened and traversed by disrupted anchoring filaments. In the stroma, interfibrillar collagen spacing was increased and abnormally large PG were present. Descemet's membrane (DM) contained lucent spaces in which there were small filaments. Keratocyte and endothelial cells contained melanin granules. A posterior collagenous layer (PCL) contained numerous microfilaments and wide spacing collagen fibres with a periodicity of 100 nm. Large quantities of abnormal PG were observed at the endothelial face of the PCL. Very strong labelling with  $\beta$ ig-h3 antibody was observed in the basement membrane, Bowman's layer, stroma, DM, and PCL, but not in keratocytes and endothelial cells. Strong labelling with BC10 and TN2 was seen below the epithelium, in electron lucent spaces where the hemidesmosomes were absent, in the fibrotic pannus, in parts of Bowman's layer, the stroma, and Descemet's membrane. Labelling with BC10 was stronger and more evenly distributed than with TN2. Fibrillin-1 (MAB2502) and fibrillin (MAB1919) labelling was similar to TN-C labelling. Fibrillin (MAB1919) labelling was stronger than fibrillin-1 (MAB2502) labelling.

**Conclusions**—Immunoelectron microscopy showed precise labelling of proteins at both the cellular and the subcellular level. Expression of proteins  $\beta$ ig-h3, TN-C, fibrillin, and fibronectin was highly increased compared with normal cornea. In the oedematous stroma, increased collagen fibril separation may facilitate a wider distribution of some soluble proteins, such as  $\beta$ ig-h3, throughout stroma. The modified expression of the proteins studied in these cases of BK may be regarded as part of an injury response.

(Br J Ophthalmol 2001;85:720–731)

Post-surgical bullous keratopathy is a leading indication for keratoplasty. Both aphakic and phakic BK are due to endothelial dysfunction, giving rise to epithelial bullae and stromal oedema resulting in loss of transparency. Ultrastructural changes in BK have been reported by various authors.<sup>1–3</sup> Immunohistochemically, it has been shown that BK is associated with the expression of TN-C,<sup>4,5</sup> fibronectin, fibrillin,<sup>4,6</sup> and  $\beta$ ig-h3.<sup>7</sup>

$\beta$ ig-h3 is an extracellular matrix protein that was first detected in a human lung adenocarcinoma cell line after stimulation by TGF- $\beta$ .<sup>8</sup> Recently, specific missense mutations have been reported in the  $\beta$ ig-h3 gene (transforming growth factor  $\beta$  induced gene) in four autosomal dominant corneal dystrophies—that is, lattice type I, granular, Avellino, and Reis-Bückler's corneal stromal dystrophies.<sup>9</sup>  $\beta$ ig-h3 has been immunohistochemically localised to numerous body tissues, particularly within the basement membrane of skin and interstitial tissue.<sup>10,11</sup>

TN-C is a large hexameric glycoprotein composed of multiple domains.<sup>12–14</sup> It is one of a family of four proteins, tenascin-cytotactin (TN-C), tenascin-restrictin (TN-R), tenascin-X (TN-X), and tenascin-Y (TN-Y) derived from different gene products.<sup>14–17</sup> They play an important part in many dynamic cellular activities. In humans, TN-R is restricted to the central nervous system and TN-Y has been described only in the chicken.<sup>12,14,18</sup> TN-C is the product of a single gene localised within region q32-q34 of chromosome 9.<sup>19,20</sup> However, alternative mRNA splicing gives rise to a number of variants which are associated with the mediation of a wide range of cellular properties, such as adhesion,

Department of  
Optometry and Vision  
Sciences, Cardiff  
University, Cardiff, UK  
S Akhtar  
K M Meek

Nuffield Department  
of Ophthalmology,  
University of Oxford,  
Oxford, UK  
A J Bron

Royal Glamorgan  
Hospital, Llantrisant,  
UK  
N R Hawksworth

Academic Department  
of Ophthalmology,  
Manchester Royal Eye  
Hospital and  
University of  
Manchester,  
Manchester, UK  
R E Bonshek

Correspondence to:  
Dr Saeed Akhtar,  
Department Optometry and  
Vision Sciences, Cardiff  
University, Redwood  
Building, Kings Edward VII  
Avenue, PO Box 905, Cardiff  
CF10 3NB, UK  
AkhtarS@Cardiff.ac.uk

Accepted for publication  
12 February 2001

Table 1 Clinical data of pseudophakic/aphakic bullous keratopathy (PBK/ABK) patients

Specimen	Age (years)	Sex	Clinical details	Diagnosis
1	61	Female	Endothelial decompensation following cataract extraction	ABK/PBK
2	86	Female	Radial iridotomy and trabeculectomy	BK with pseudophakia and pupilloplasty
3	76	Male	Anterior chamber lens and subsequent corneal decompensation	PBK
4	85	Female	Anterior chamber lens and subsequent corneal decompensation	PBK
5	76	Female	Anterior chamber lens and subsequent corneal decompensation	PBK

anti-adhesion, migration, proliferation, and differentiation.<sup>21–23</sup> TN-C is expressed in the human cornea in development, healing and repair, and inflammation and scarring.<sup>24–27</sup> In addition, a number of studies have documented expression of TN-C and its variants in bullous keratopathy.<sup>4–5</sup>

Fibrillin-1 (FBN1) is a high molecular weight glycoprotein found in virtually all extracellular matrices.<sup>28–30</sup> Mutation in the FBN1 gene that encodes fibrillin is responsible for Marfan syndrome, an autosomal dominant, connective tissue disorder, that affects the cardiovascular and musculoskeletal system, as well as the eye.

In the present paper, we report for the first time the immunoelectron localisation of the proteins  $\beta$ ig-h3, tenascin-C (clone TN-2 and BC10), fibrillin-1, and fibronectin with reference to the detailed ultrastructural morphology of bullous keratopathy corneas.

### Methods

A normal corneal button was obtained 24 hours post mortem and three BK corneal buttons were obtained within 30 minutes of penetrating keratoplasty and were fixed immediately. Two more buttons were obtained from archived material (2 years old) by processing wax blocks through xylene and a graded series of ethanol (see Table 1).

All the corneas were divided into three parts. The first part was immersed in 3% glutaraldehyde in 0.1M phosphate buffer for 2 hours and post-fixed in 1% osmium tetroxide in 0.1M phosphate buffer for a further hour. The second part was fixed in 3% glutaraldehyde containing 0.05% cuprolinic blue (BDH Ltd, Dorset) using a critical electrolyte concentration mode. The tissue was then dehydrated through a graded ethanol series and embedded in Spurr resin. Semithin (1  $\mu$ m) sections were stained with toluidine blue for light microscopy. Ultrathin sections were stained with uranyl acetate and lead citrate, and observed by transmission electron microscopy (Jeol 1010; Jeol Ltd, Akishima, Japan).

The third part (less than 1 mm<sup>3</sup>) was fixed in freshly prepared 4% paraformaldehyde (PFA) in 0.1M phosphate for 2 hours at 4°C. Tissue was washed three times (15 minutes) in 0.1M PBS, and dehydrated in 30%, 50% (4°C), and in 70%–100% ethanol (–20°C) (1 hour in each). Tissues were infiltrated at –20°C in two 1 hour changes of a mixture of 100% ethanol and LR white (–20°C) and three 8 hour changes of LR white (–20°C). They were

finally polymerised in LR white at –20°C for 48 hours under ultraviolet light. Ultrathin sections were cut from the blocks and collected on 200 mesh formvar-carbon nickel grids.

### IMMUNOELECTRON MICROSCOPY

Polyclonal, rabbit, anti-human  $\beta$ ig-h3 antibody was a gift from Dr K Bennett, Bristol Myers Squibb, USA. The monoclonal antibodies: mouse anti-human tenascin, BC10, (MAB 1918), mouse anti-human fibrillin-1 (MAB 2502), and mouse anti-human-fibrillin (MAB 1919), were obtained from Chemicon, International, UK. Monoclonal mouse anti-human tenascin, TN2, (MO636) and polyclonal rabbit anti-human fibronectin were obtained from Dako Ltd, UK. The specificity of the antibody to human antigens was tested and confirmed by the supplier with immunological assays. Antibodies were visualised with 10 nm goat anti-mouse and goat anti-rabbit immunogold conjugate. The immunogold conjugates, goat serum, bovine serum, and Tween-20 were supplied by Biocell, Cardiff, UK.

Sections were treated at room temperature by floating on a 50  $\mu$ l drop of phosphate buffered saline (PBS) containing 0.1% bovine serum albumin (PBS-BSA) for 15 minutes, followed by PBS-BSA containing 5% normal goat serum for 30 minutes. They were incubated overnight in primary antibody, rabbit anti-human  $\beta$ ig-h3 (1:50 to 1:500), mouse anti-human tenascin, BC10, (MAB 1918) (1:50 to 1:500), mouse anti-human tenascin, TN2, (MO636) (1:25), mouse anti-human fibrillin-1 (MAB 2502), anti-human fibrillin MAB 1919 (1:50 to 1:500), and rabbit anti-human fibronectin (1:50). To remove unbound antibody, sections were washed with 0.05 M TRIS buffered saline (TBS) pH 7.4 (three washes, 5 minutes each), TBS pH 7.4 containing 0.2% BSA (three washes, 5 minutes each) and TBS pH 8.4 containing 1% BSA for 3  $\times$  5 minutes. Sections were then incubated in secondary antibody-10 nm immunogold conjugate diluted 1:25 in TBS pH 8.4 containing 1% BSA for 50 minutes. The unbound secondary antibody was removed by washing in TBS-BSA (three washes, 5 minutes each), PBS, and distilled water (three washes, 5 minutes each). In all experiments, immunoelectron controls were performed by substituting normal goat serum for the primary antibody. The immunoreaction was repeated three times with three replicates for each antibody used. Normal tissue was processed in parallel as a control. Sections were stained with 2% aqueous uranyl acetate and lead citrate and examined in a Jeol 1010 transmission electron microscope.

### Results

Ultrastructural findings and immunolocalisation of proteins in all BK corneas were similar.

#### EPITHELIUM

Epithelial cells were degenerate and had numerous large vacuoles, especially around the nucleus (Fig 1A). There were large lucent spaces inside most basal epithelial cells, above Bowman's layer (Fig 1B), many of which

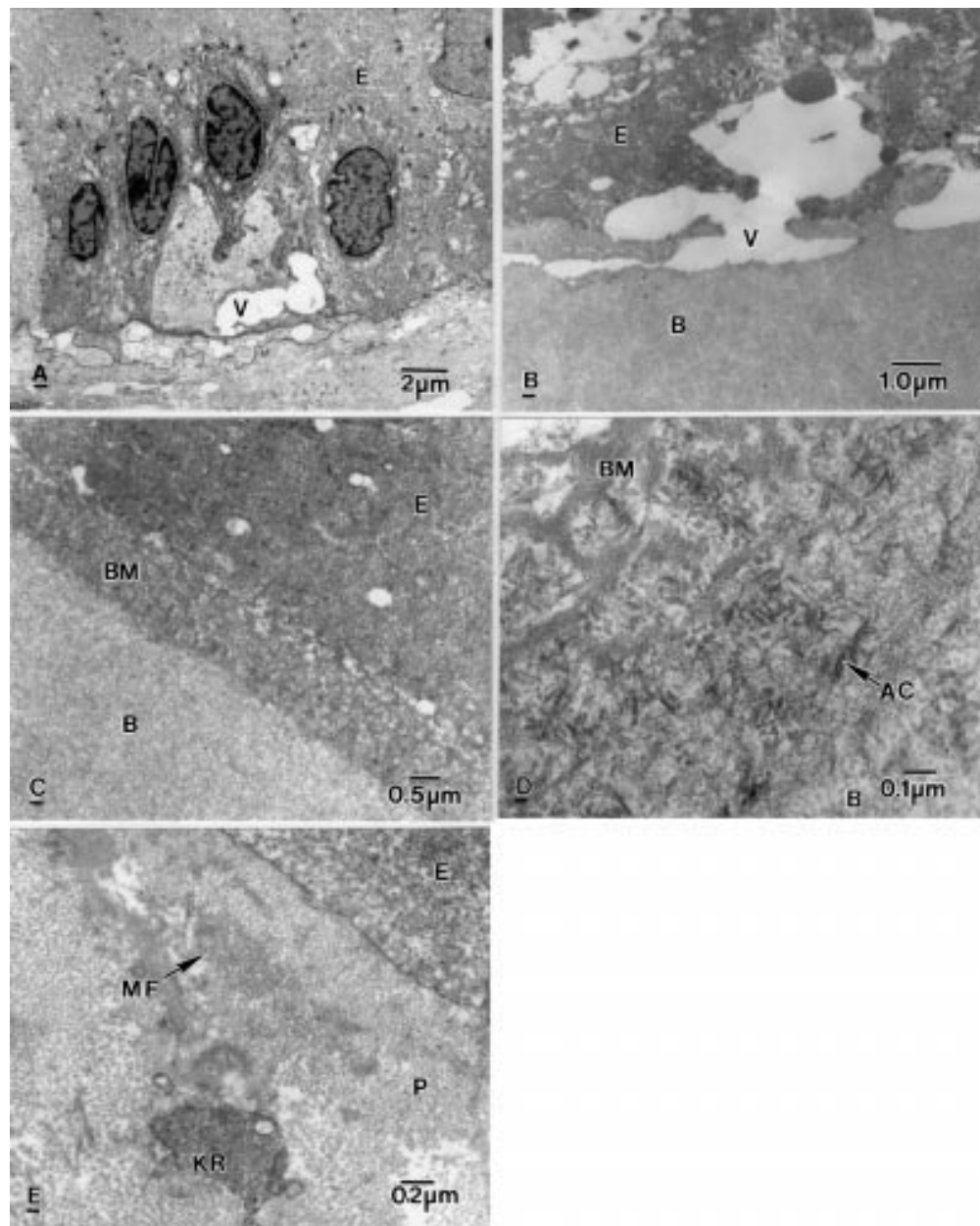


Figure 1 Electron micrographs showing ultrastructural alteration in a bullous keratopathy cornea. (A) Electron lucent vacuole (V) in a degenerate basal epithelial cell (E) and vacuoles in the subepithelial region. (B) Subepithelial vacuole (V) between an epithelial cell (E) and Bowman's layer (B). (C) Thick basement membrane (BM) between epithelial cells (E) and Bowman's layer (B). (D) Basement membrane (BM) containing anchoring filaments (AC) above Bowman's layer (B). (E) Subepithelial pannus (P) containing microfilaments (MF) and rounded keratocytes (KR).

coalesced to form extensive subepithelial bullae. Hemidesmosomes were often absent or degenerate. The subepithelial basal lamina (1.5–2 µm thick) was thickened, showing a grid-shaped structure with disrupted anchoring filaments (40–120 nm long) ((Figs 1C, D). In some places, the subepithelial region was infiltrated by thick fibrotic tissue (1 µm thick) containing microfilaments, basement membrane material, and remnants of keratocytes (Fig 1E), below which was either a normal looking Bowman's layer (7 µm) or a degenerate Bowman's layer containing rounded electron dense material.

Small folds of epithelium were present, which contained basal laminar material with numerous disrupted anchoring filaments (Fig

2A–C). Occasionally, below an electron dense basal lamina, degenerate keratocytes lined up in a single layer within fibrotic tissue (Fig 2A). The degenerate keratocytes appeared to be migrating into the base of each fold (Fig 2B).

#### STROMA

In some regions of the stroma, the separation of collagen fibrils was greater than normal and the interfibrillar space contained a network of very fine filaments. There were electron lucent lakes throughout the stroma. Wavy collagen lamellae were prominent in the pre-Descemet's stroma and around the pre-Descemet's spaces (Fig 2D). Wavy lamellae were also seen in other parts of stroma. Wide spacing collagen fibrils were observed just below the epithelium

in a degenerate fibrotic pannus and in the posterior stroma. Groups of microfilaments were seen in some parts of the stroma, especially adjacent to Descemet's membrane (DM) (Fig 3C).

#### DESCEMET'S MEMBRANE AND POSTERIOR COLLAGENOUS LAYER

Descemet's membrane (DM) was 8–10  $\mu$ m thick and was differentiated into banded and non-banded zones. The non-banded zone had numerous lucent spaces which contained small filaments. A prominent banding pattern similar to banded DM, was occasionally seen in the middle of the homogeneous DM. In the DM of all corneas, there were electron lucent cracks or breaks, scrolls of Descemet's material, and

nodule formation with the appearance of Hassal-Henle warts. These contained degenerate collagen fibrils (Fig 3A, B). The posterior collagenous layer (PCL) contained numerous groups of microfilaments and very prominent wide spacing fibres with a periodicity of 100 nm (Fig 3C) embedded in basement membrane-like material. The bands of wide spacing fibrils were connected by very thin microfibrils. Collagen fibrils were degenerate and sparse, and were distributed between large, lucent spaces. Some endothelial cells were present on the posterior surface of the posterior collagenous layer, but in most regions, no cells were present. Where endothelial cells were observed, the cytoplasm was dense, with prominent rough endoplasmic

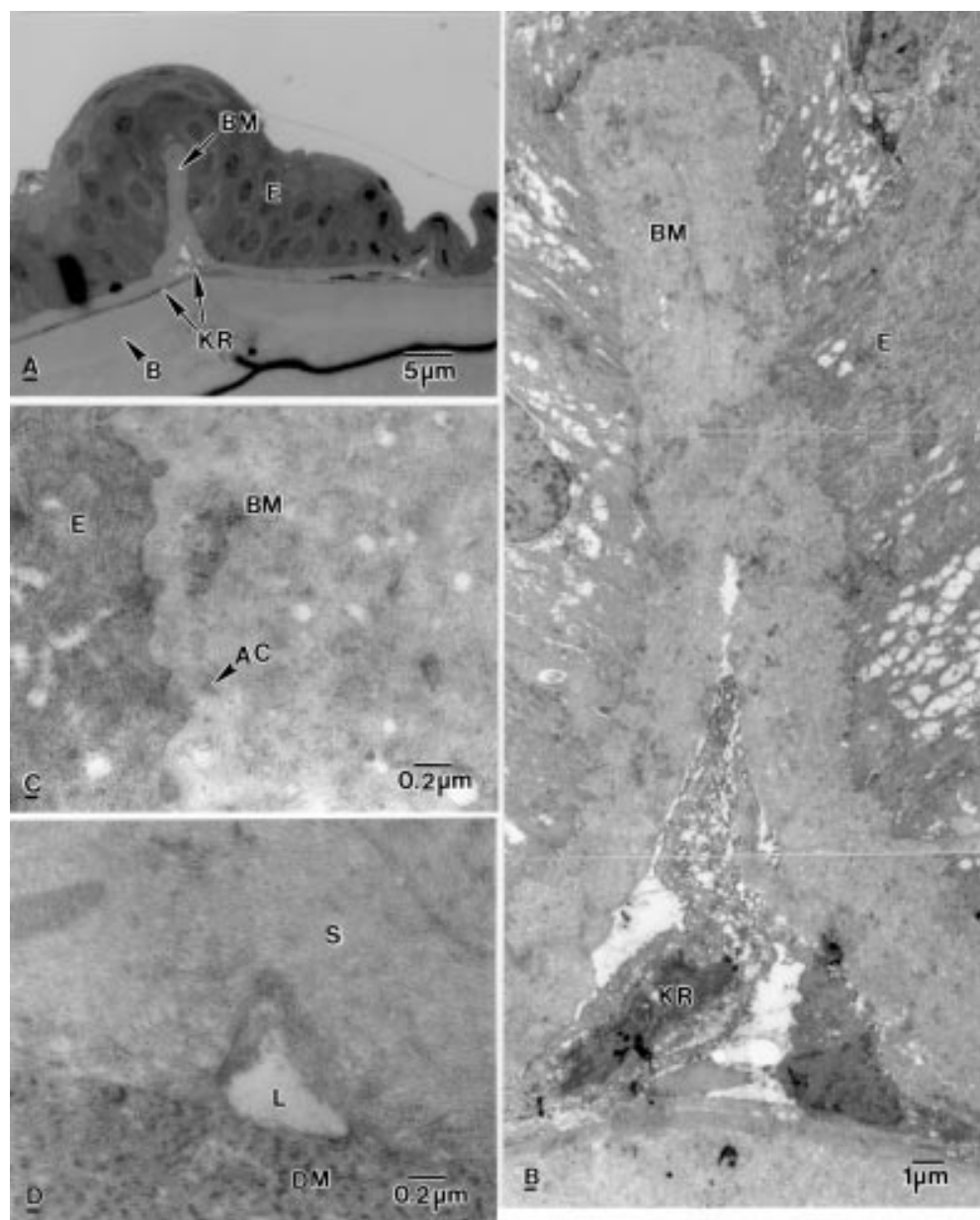


**Figure 2** Light and electron micrograph of bullous keratopathy cornea. (A) Epithelial fold containing basement membrane material (BM). Keratocytes (KR) are arranged in a line above Bowman's layer (B) and the anterior stroma. (B) High magnification of the epithelial fold shown in (A). Keratocytes (KR) are present in the epithelial fold which contains basement membrane material (BM). (C) Part of an epithelial fold showing disrupted anchoring filaments (AC) in basement membrane material (BM). (D) Electron lucent lake (L) between the stroma (S) and Descemet's membrane (DM).

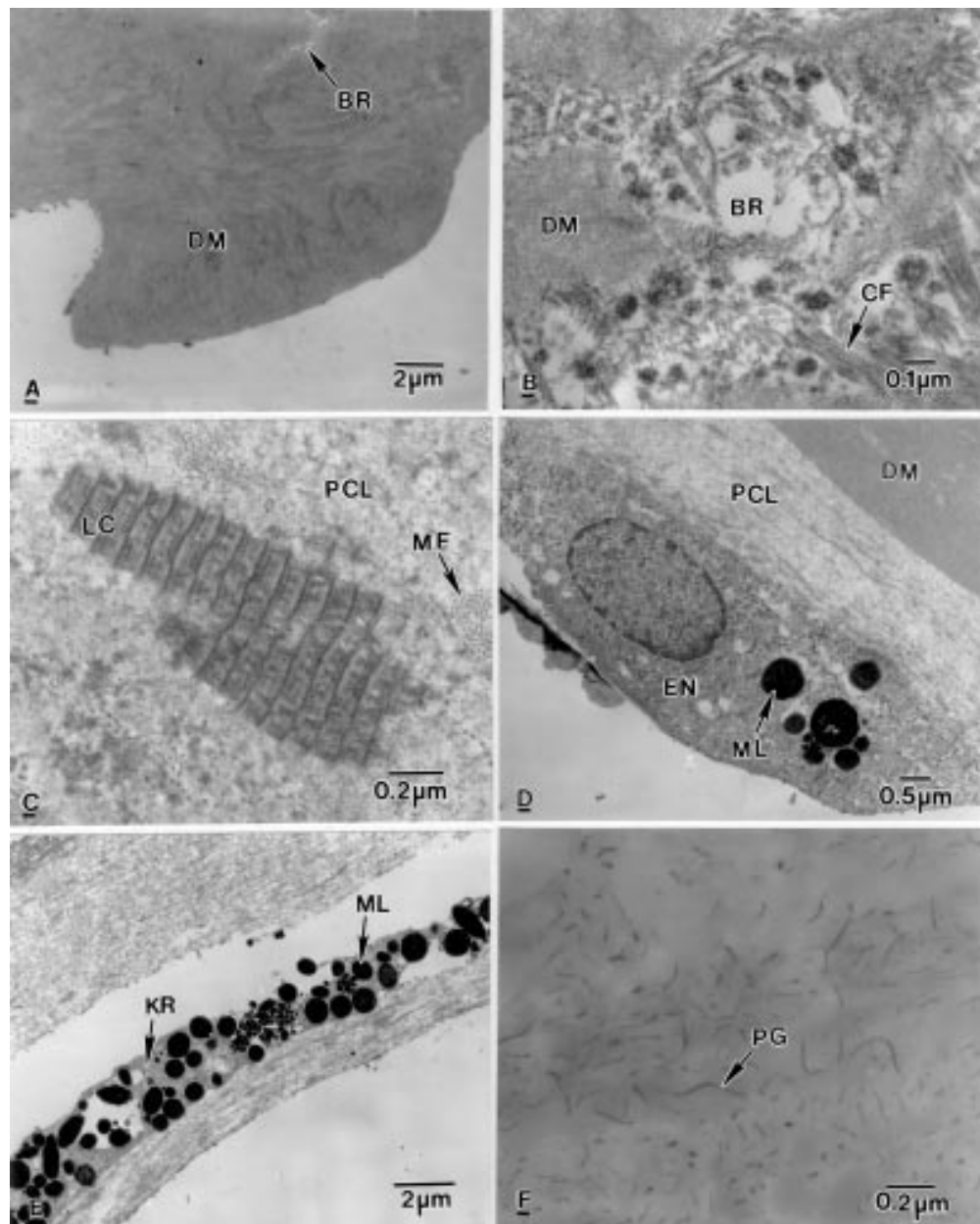


**Figure 3** Electron micrographs of the posterior part of bullous keratopathy corneas. (A) Part of Descemet's membrane (DM) with a break (BR). (B) Collagen fibres (CF) and electron dense material in a break (BR) present in Descemet's membrane (DM). (C) Posterior collagenous layer (PCL) containing wide spacing collagen (LC) and microfilaments (MF). (D) Below the PCL, an endothelial cell (EN) containing melanin granules (ML). (E) A degenerate keratocyte (KR) containing melanin granules (ML). (F) Part of anterior stroma containing abnormal proteoglycans (PG).

reticulum and melanin granules (Fig 3D). Other cell organelles were not well differentiated.

#### KERATOCYTES

Degenerate keratocytes were observed in the fibrotic pannus and in the PCL, and they were also scattered throughout the stroma. Some of the keratocytes in the fibrotic pannus were rounded in shape (Fig 1F). In degenerate keratocytes, the cytoplasm was either disintegrated or had become a homogeneous mass, containing large vacuoles and melanin granules (Fig 3E). Nuclei were often apoptotic.

#### PROTEOGLYCANS

Proteoglycans (PG) in the basement membranes and anterior stroma were abnormally

large (200–300 nm) (Fig 3F). Some aggregates of these large PG filaments were observed just below the basal epithelial cells where hemidesmosomes were absent. In some regions of the posterior stroma, PG were also very large (180 nm). Large PG filaments were also present around electron lucent lacunae throughout the stroma. In the middle and, posterior stroma and the PCL, PG filaments were found in large quantities, but their size was smaller (100 nm). A large quantity of abnormal PG was observed at the endothelial face of the PCL.

#### $\beta$ IG-H3

In normal corneal samples, moderate labelling was observed in the subepithelial basement

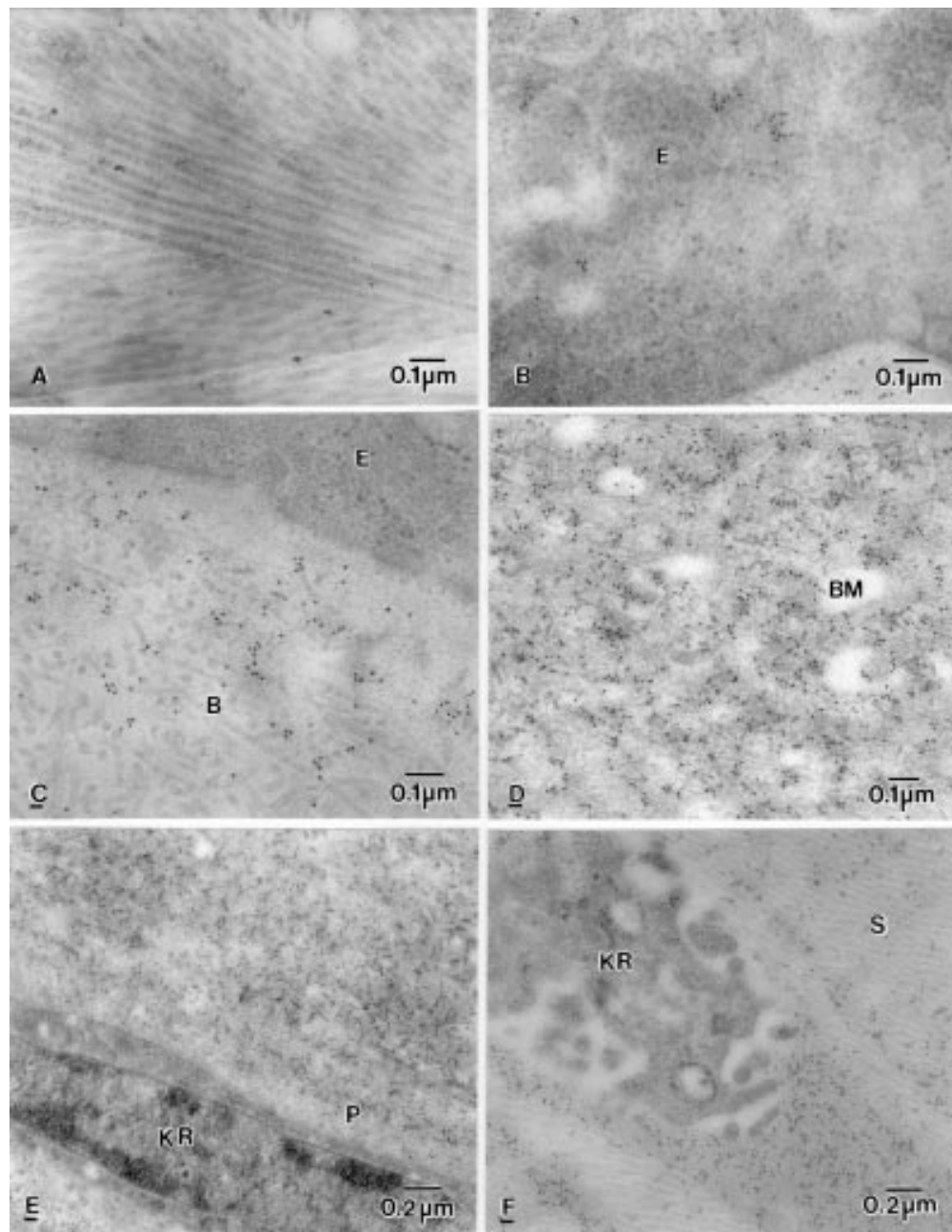


Figure 4 Electron micrograph showing labelling of  $\beta$ ig-h3 in BK corneas. (A) Control for immunoreaction. (B) Clumped labelling in epithelial cell (E). (C) Moderate clumped labelling in normal looking Bowman's layer (B). (D) Heavy labelling in basement membrane (BM) and around disrupted anchoring filaments. (E) Diffuse labelling on fibrotic pannus tissue (P) but not in the keratocyte (KR). (F) No labelling in the keratocyte (KR). (F) No labelling in the keratocyte (KR) but heavy labelling close to the keratocyte (KR) in the anterior stroma (S).

membrane, Bowman's layer, and stroma. Labelling was strong in patches of fibrillar material near keratocytes but scanty around the keratocytes themselves. Dense labelling was seen in Descemet's membrane, but not in or close to the endothelium. Labelling was absent from the epithelial cells and keratocytes.

In the BK specimens, a small amount of labelling for  $\beta$ IG-H3 was observed in the epithelial cells (Fig 4B), in the degenerate Bowman's layer, and in the normal looking Bowman's layer (Fig 4C). In some parts of Bowman's layer, labelling was dense. Labelling was strong in the thick basement membrane, especially around the disrupted anchoring filaments (Fig 4D) and also within epithelial folds.

Below the basement membrane, fibrotic pannus tissue was heavily labelled, while keratocytes were not (Fig 4E, F). Labelling was moderate in the anterior, middle, and posterior stroma but there were also some more strongly labelled patches. The electron dense material around degenerate collagen fibrils (Fig 5A) and the fibrillar material distributed throughout the stroma was very strongly labelled with the antibody (Fig 5B). Fibroblasts, keratocytes, and lucent areas around keratocytes were not labelled, but the fibrillar (or fibrous) material (described earlier) adjacent to the keratocytes was very strongly labelled with the antibody (Fig 5C). Banded DM was heavily labelled whereas homogeneous, non-banded DM was

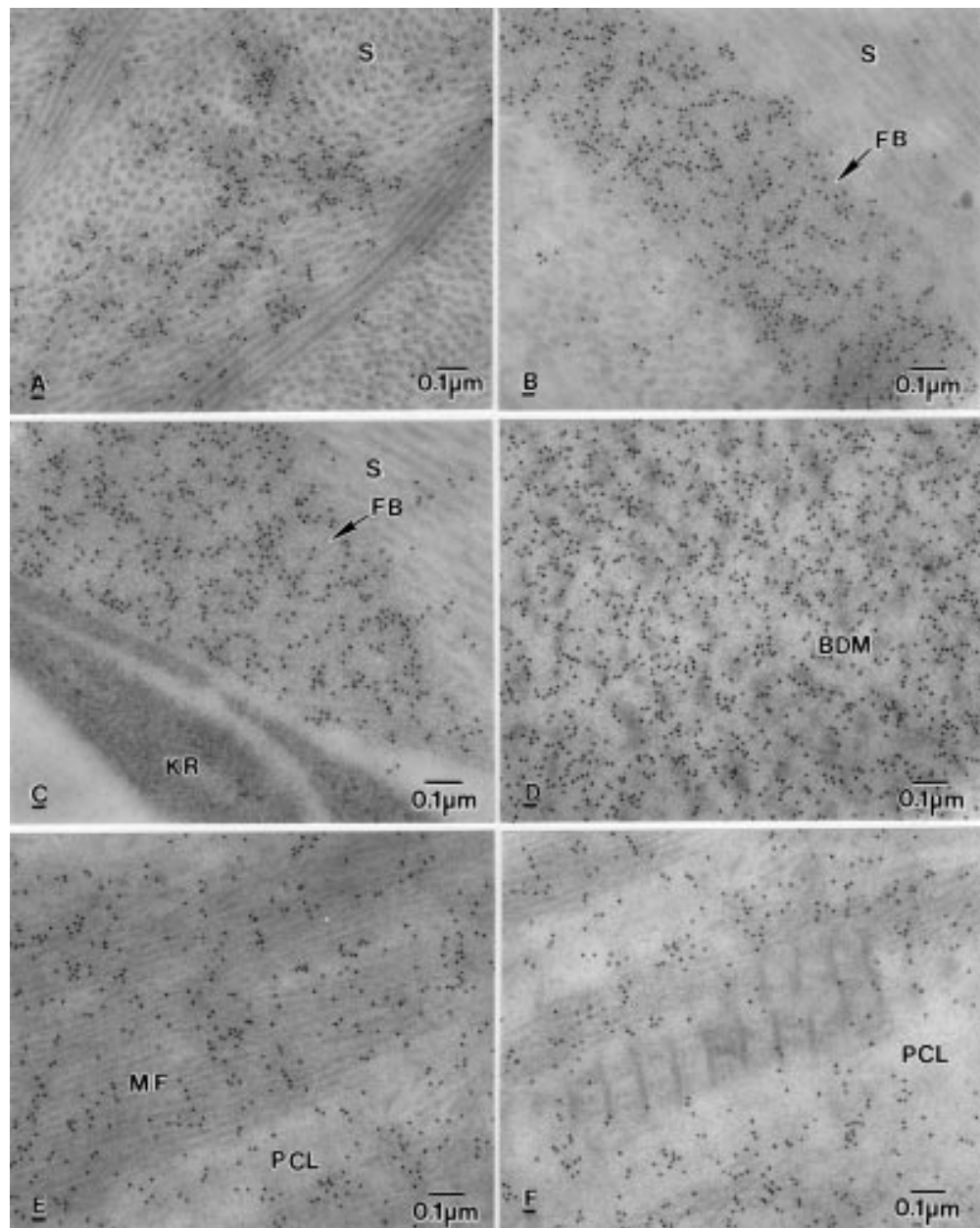


Figure 5 Electron micrograph showing labelling of big-h3 in BK corneas. (A) Labelling on electron dense material present among collagen fibrils in the anterior stroma (S). (B) Labelling on fibrous (or fibrillar) material (FB) in the posterior stroma (S). (C) Labelling on fine fibrous (or fibrillar) material (FB) close to degenerate keratocyte (KR) but not in the keratocyte in the middle stroma (S). (D) Heavy labelling on banded Descemet's membrane (BDM). (E) Labelling on microfilaments (MF) in the PCL. (F) Labelling on electron dense material but not wide spacing collagen in the PCL.

only moderately labelled (Fig 5D). In the PCL, microfilaments, and basement membrane material were heavily labelled (Fig 5E, F). Wide spacing collagen and lucent spaces in the PCL were not labelled. Endothelial cells, when present, were not labelled, but the endothelial face of the PCL had moderate labelling.

#### TENASCIN-C

Labelling of BC10 was seen in the squamous (Fig 6A), wing, and basal epithelial cells. Strong labelling was seen in electron lucent spaces where the hemidesmosomes were absent and in the fibrotic pannus tissue, especially in the region where degenerate anchoring filaments were seen (Fig 6B). Diffuse labelling was observed in Bowman's layer (Fig 6C) and

throughout the stroma (Fig 6D). Labelling was very strong in the pre-Descemet's stroma and in the banded DM, especially close to the slit-like lucent spaces (Fig 6E). The labelling was also seen in the PCL (Fig 6F) and on the endothelial face of the PCL.

A small amount of labelling TN2 of tenascin was observed on the surface of the epithelium and in epithelial cells. Some staining was seen around degenerate keratocytes in the anterior stroma. Clumped labelling was seen in the fibrotic pannus tissue below the epithelium, in the anterior stroma beneath Bowman's layer, and in the posterior stroma close to Descemet's membrane. No staining was seen in the middle stroma or in the banded Descemet's membrane. Labelling was particularly high in the

homogeneous middle and lower parts of the non-banded DM and in the PCL.

#### FIBRILLIN

The labelling with fibrillin-1 clone MAB 2502 was observed on the very fine electron dense fibrillar material both on the surface and within the epithelial cells (Fig 7A). The labelling was prominent in the pannus on fine microfilaments close to degenerate keratocytes (Fig 7B) and in the anterior stroma (Fig 7C). Labelling was also seen in DM and the PCL on very fine microfibrils close to the endothelium. Labelling with fibrillin clone MAB 1919 was similar to that with fibrillin-1 clone MAB 2502, but was more intense, especially in DM (Fig 7D). It was also observed in the middle and posterior stroma.

#### FIBRONECTIN

Labelling for fibronectin was observed on the surface of epithelial cells (Fig 7E) and within the epithelial cells, close to the lucent spaces. The labelling was also observed in the nucleus and close to the nucleus and on the nuclear membrane of the epithelial cells. The part of the basement membrane that was attached to the epithelial face was labelled with antibody, and there was also some labelling in Bowman's layer. In the anterior, middle, and posterior stroma, large portions of the longitudinally running collagen fibrils were labelled with the antibody (Fig 7F). The cytoplasm and nucleus of the keratocytes in the stroma had prominent labelling. The middle and endothelial faces of DM and the fibrocellular layer also had

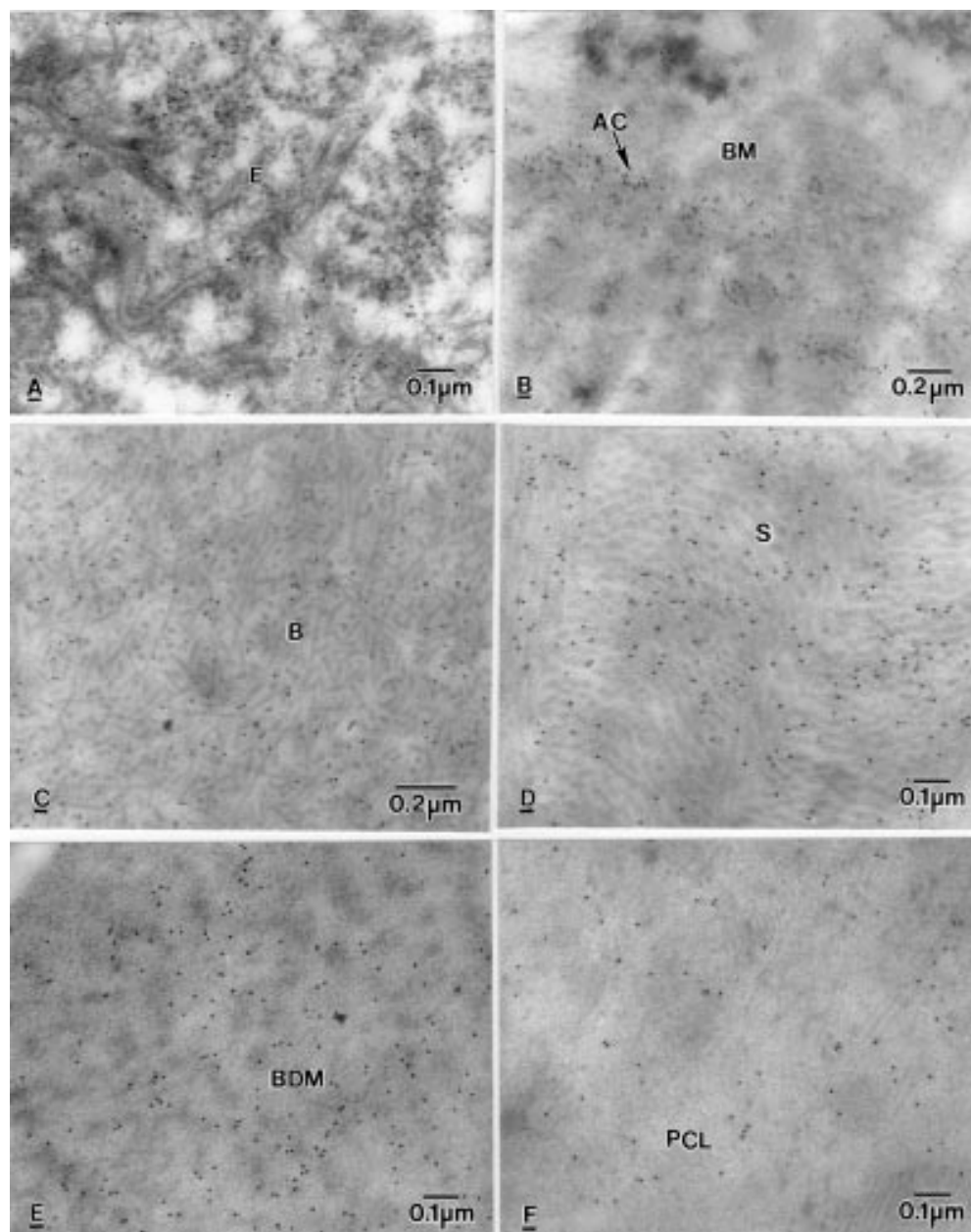


Figure 6 Electron micrographs of BK corneas showing labelling of BC10, in (A) epithelium (E), (B) Basement membrane (BM) and around anchoring filaments (AC), (C) Bowman's layer (B), (D) stroma (S), (E) banded Descemet's membrane (BDM), (F) posterior collagenous layer (PCL).



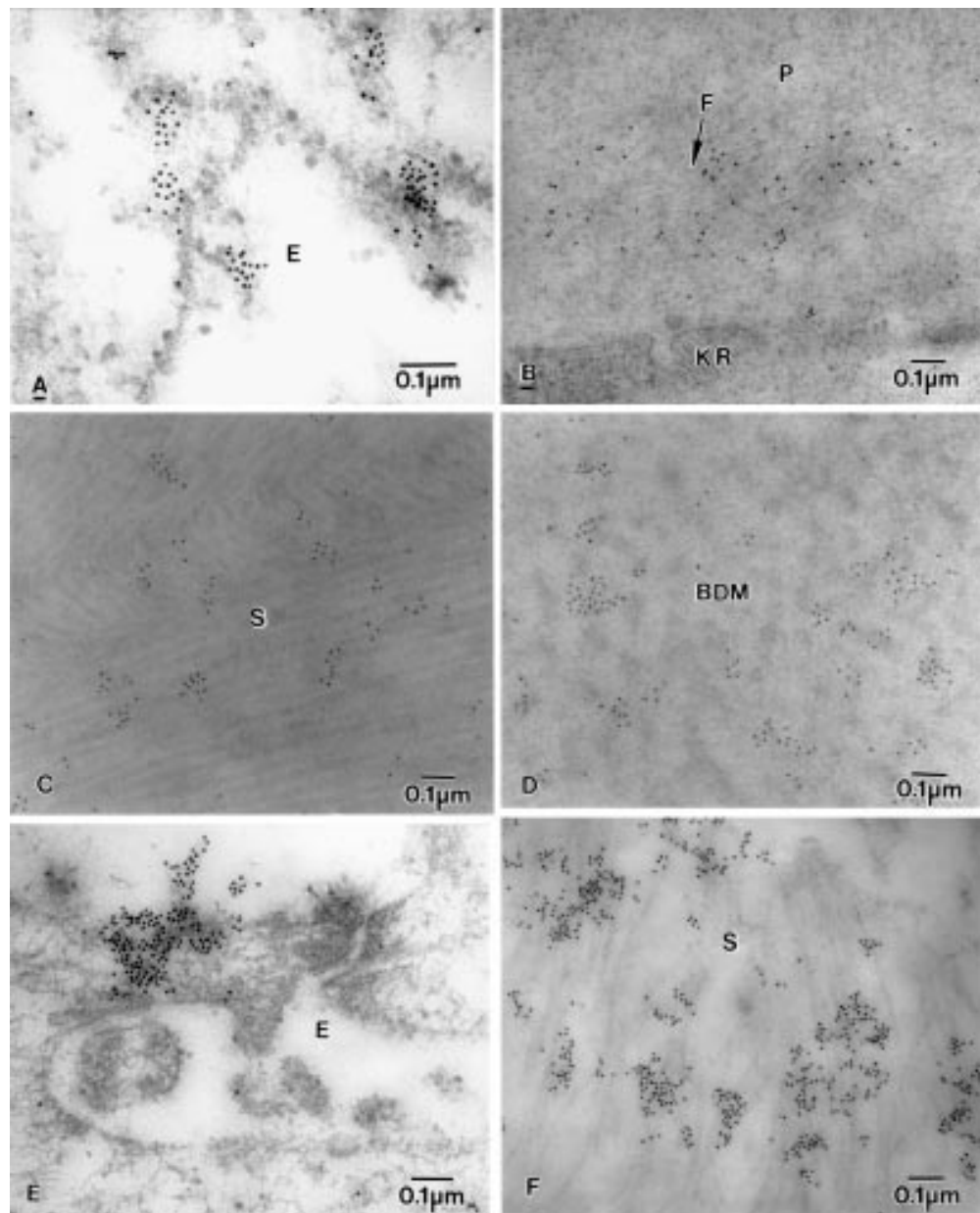


Figure 7 Electron micrograph of BK corneas showing labelling of fibrillin-1-MAB2502, fibrillin-MAB1919, and fibronectin. (A) Fibrillin-1-MAB2502 labelling in epithelial cell (E), (B) diffuse labelling of fibrillin-1-MAB2502 on microfibrils (F) near a degenerate keratocyte (KR) in the pannus (P). (C) fibrillin-MAB1919 labelling on collagen fibrils in stroma (S), (D) Fibrillin-MAB1919 labelling on banded Descemet's membrane (BDM). (E) Labelling of fibronectin on the surface of the epithelium (E), and (F) in the stroma (S).

electron dense patches labelled with the antibody.

### Discussion

In post-surgical bullous keratopathy, injury causes a focal or diffuse disturbance of the endothelium. Cell loss, where it occurs, is followed by spreading of cells from the adjacent areas of the endothelium. Where endothelial loss is extreme, or where further losses occur with the passage of time, the resulting endothelial sheet may no longer be able to perform its normal function of deturgescing the cornea, and corneal oedema results, with or without the formation of epithelial bullae. Where the rate of endothelial

cell loss is so high that the remaining endothelial cells are unable to cover the whole area of the posterior cornea, the remaining endothelial cells lose their normal appearance and function, and become flat or attenuated.<sup>6</sup> This was confirmed in the present study by LM and TEM. The disordered endothelial sheet, perhaps containing cells of fibroblastic origin, lays down a posterior collagenous layer which may be banded, fibrillar, or fibrocellular.

We have confirmed earlier observations that endothelial damage causes nodulation, breaks, and scroll formation in DM.<sup>6</sup> Abnormal endothelial function probably including fibroblastic activity, produces a posterior collagenous layer containing wide spacing collagen,

microfilaments and basement membrane-like material.<sup>7</sup> The functional failure of the endothelial cells leads to corneal oedema and formation of bullae in the epithelium and subepithelial region.

Endothelial decompensation leads to an increase in stromal thickness and to subepithelial fibrosis with an accumulation of abnormal PG<sup>31</sup> and degenerate collagen fibrils. It is believed that the degenerate pannus is formed when fibroblast-like cells, derived from the corneal stroma, insinuate themselves into the space between Bowman's membrane and the epithelial basement membrane.<sup>32</sup> Keratocyte numbers are reported to be reduced in bullous keratopathy.<sup>6</sup> Since the nutrition of keratocytes would be anticipated to be relatively uninfluenced by the swelling, another mechanism must be sought their loss. One suggested mechanism is an involvement of the epithelium in an IL-1, Fas/Fas ligand induced mechanism of apoptotic death.<sup>33</sup>

Kenny *et al*<sup>5</sup> believe that the fibrotic pannus is a response to the formation of epithelial bullae. This is thought to lead to epithelial degeneration, reduplication, and the synthesis of an intraepithelial basal lamina-like material, within epithelial folds. Eagle *et al*<sup>2</sup> suggested that folded epithelial bullae are probably caused by buckling of the basement membrane due to a shift or dislocation of the loosened or shallowly detached corneal epithelium. The abnormal function of the epithelium produces a multilayered basal lamina, and loss of hemidesmosomes results in disruption of the anchoring filaments.

Immunoelectron microscopy has shown for the first time the precise labelling of proteins at the cellular and subcellular level which could not be shown by light microscopy or by any other technique. This ultrastructural localisation of the proteins has provided us with a better understanding of their involvement in BK corneas:

#### $\beta$ IG-H3

In our normal corneal samples, labelling was observed in the subepithelial basement membrane, Bowman's layer, stroma, and Descemet's membrane, but not in or close to the endothelium. Similar labelling of  $\beta$ ig-h3 was observed by Streeten *et al*.<sup>34</sup> Takács *et al*<sup>11</sup> reported that, in normal cornea, labelling was strong in the basal epithelial cell layer and endothelium, faint in the stroma and keratocytes, and absent in Bowman's layer and DM. This differs from our findings in BK, where labelling was scanty in the epithelial cells, and heavy in the thick basement membrane, on the anchoring filaments, in some parts of the stroma and on the very fine fibrous material around keratocytes. Labelling was not seen within keratocytes. Absence of labelling in keratocytes suggests that most of the  $\beta$ ig-h3 protein has been secreted from the epithelium and deposited on the fibrous material. Labelling was also strong on fibrous material in the stroma, in DM, and on microfilaments in the PCL but it was not seen in the endothelium. Most of the stroma had moderate labelling.

Takács *et al*<sup>11</sup> reported that in PBK, there was positive labelling of the basal epithelial layer, under the epithelium, in and above the endothelium, and in the keratocytes, contrary to our observations. They also found staining in the fibrotic area—that is, the pannus and PCL, similar to our findings.

The association of  $\beta$ ig-h3 with extracellular matrix macromolecules, such as fibrillin in microfibrils,<sup>35</sup> type II collagen in cartilage,<sup>36</sup> and type VI collagen in cornea<sup>37,38</sup> has suggested that  $\beta$ ig-h3 functions as an extracellular matrix molecule, perhaps facilitating cell-matrix interactions during morphogenesis.<sup>14,37</sup>  $\beta$ ig-h3 is found in rabbit corneal epithelial cells,<sup>39</sup> and both in the corneal epithelium and endothelium, as well as in the newly formed extracellular matrix of Fuchs' dystrophy cornea.<sup>40</sup> It is likely that in the oedematous stroma of BK, the distribution of  $\beta$ ig-h3 across the stroma is facilitated by the widening of intercollagenous fibrillar spaces.<sup>41</sup>

The presence of TGF- $\beta$ 1, TGF- $\beta$ 2, and cytokines (IFN- $\gamma$ , IL-2, IL-4, IL-10, IL-12) was shown in bullous keratopathy corneas, and scarring often accompanies this disease.<sup>42</sup> Furthermore, TGF- $\beta$ , which has an important role in wound healing, is considered to be the major factor for enhancing the secretion of  $\beta$ ig-h3.<sup>11</sup> It is believed that TGF- $\beta$  promotes the secretion of  $\beta$ ig-h3 in BK corneas. Since it has been found in several cell types,<sup>14,42</sup> it is believed that this protein ( $\beta$ ig-h3) could also play an important part in cellular adhesion and/or signalling<sup>11,21</sup> like other proteins such as TN-C and fibrillin.<sup>8,9,11</sup>

#### TENASCIN-C

From our observations, labelling of TNC by TN-2 and BC10 was found in the fibrotic pannus and PCL, anterior stroma and pre-Descemet's posterior stroma, and in non-banded DM, similar to the observation of Ljubimov *et al*.<sup>8</sup> In addition, however, BC10 labelling was also found within epithelial cells, in the basement membrane around disrupted anchoring filaments, in Bowman's layer, and in banded DM close to electron lucent spaces.

Ljubimov *et al*<sup>8</sup> have suggested that following injury, mechanical stress on myofibroblasts induced by stromal swelling, causes contraction which acts on the surrounding collagen fibrils, and tends to compress the normal structure of the stroma, which results in the production and deposition of TNC.<sup>8</sup> In cultures, contraction of myofibroblasts induces the production and deposition of TNC.<sup>16</sup> Maseruka *et al*<sup>25</sup> have also demonstrated persistent TNC expression in corneas at sites of tension in malapposed corneal grafts. TNC variants have adhesive, as well as anti-adhesive properties. Using the monoclonal antibody BC2, which recognises high M<sub>r</sub> TNC variants associated (in vitro) with anti-adhesion and proliferation, Maseruka *et al*<sup>25</sup> demonstrated the presence of anti-adhesive variants along the borders of subepithelial bullae in pseudophakic bullous keratopathy corneas. BC2 is ineffective as an immunoreagent under the conditions of our ultrastructural study (data not presented)

presumably because of failure of penetration of antibody into the LR white resin embedded tissue. However, we have shown BC10 and TN2, which recognise all TNC variants, to be present in areas of loss of intercellular contacts and downregulation of focal adhesion, suggesting a role in weakening cell-substrate attachment and promotion of cell detachment by loss of intercellular contacts and downregulation of focal adhesion.<sup>16 19 43 44</sup> Thus subepithelial TN-C weakens the subepithelial adhesion contributing to the formation of bullae.<sup>41</sup> Small pH variations can modify the TN-C splicing pattern.<sup>45</sup> In addition, TNC expression can also be induced by fibrogenic cytokines<sup>46-48</sup> such as TGF- $\beta$ , fibroblast growth factor and, platelet derived growth-BB, all of which also induce the formation of  $\beta$ ig-h3.<sup>8</sup>

#### FIBRILLIN

In normal adult cornea, peripheral epithelial basement membrane showed positive staining for fibrillin-1, but little or no fibrillin-1 staining was detected in the central basement membrane.<sup>10 28 29</sup> We found no staining for fibrillin in our normal cornea.

In an earlier study of BK, fibrillin-1 was expressed in the epithelial basement membrane, the stroma, DM, the area of subepithelial fibrosis and in the PCL.<sup>10</sup> We confirmed these results and found similar fibrillin-1 staining on very fine fibrils in BK cornea. But we also found staining on the epithelial surface and inside the epithelial cells.

Fibrillin-1 accumulation has been observed during corneal wound healing.<sup>49</sup> It was also found with fibrotic extracellular matrix at Bowman's layer breaks in keratoconus corneas.<sup>5 50</sup> It is believed that fibrillin-1 accumulation in BK cornea may be part of a fibrotic, healing process occurring in these corneas, related to the altered fluid balance and corneal swelling.<sup>10</sup> It is possible that growth factors and cytokines, which are expressed during wound healing, may contribute to the appearance of fibrillin-1. An increased level of interleukins 1 $\alpha$  (IL-1 $\alpha$ ) and 8 (IL-8) in BK cornea<sup>42</sup> might be responsible for the expression of fibrillin-1 as was observed in UVB damaged skin.<sup>51</sup>

With endothelial failure, fluid accumulates in the stroma and epithelium. This results in the formation of stromal lakes or subepithelial and intraepithelial bullae and causes mechanical stress to cells in the neighbourhood of the fluid accumulation. We suggest that this, in turn, may induce epithelial cells, keratocytes, and fibroblasts in these affected areas to produce TNC,  $\beta$ ig-h3, and fibrillin as part of an injury response. It is likely that this occurs in response to the release of growth factors and cytokines, which enhance the production of the above proteins.<sup>6 25</sup> The induction of the production of anti-adhesive TNC variants,<sup>5</sup> together with  $\beta$ ig-h3 and fibrillin, contributes to the poor adhesive and growth properties of the epithelium.

We thank Dr K Bennett for the gift of  $\beta$ ig-h3 antibody. We acknowledge the financial support of the Wellcome Trust and Medical Research Council (to KMM).

- 1 Kenney MC, Chaw M. Abnormal matrix in corneas with pseudophakic bullous keratopathy. *Cornea* 1990;9:115-21.
- 2 Liu GJ, Okisa S, Mizukawa A, et al. Histological study of pseudophakic bullous keratopathy developing after anterior chamber of iris supported intraocular lens implantation. *Jpn J Ophthalmol* 1993;37:414-25.
- 3 Kenyon KR, Van Horn D, Edelhauser HF. Endothelial degeneration and posterior collagenous proliferation in aphakic bullous keratopathy. *Am J Ophthalmol* 1978;329-36.
- 4 Ljubimov AV, Saghizaden M, Spirin KS, et al. Extracellular alteration in human corneas with bullous keratopathy. *Invest Ophthalmol Vis Sci* 1996;37:997-1007.
- 5 Maseruka H, Ataullah SM, Zardi L, et al. Tenascin-cytotactin (TN-C) variants in pseudophakic/aphakic bullous keratopathy corneas. *Eye* 1998;12:729-34.
- 6 Ljubimov AV, Saghizaden M, Spirin KS, et al. Increased expression of fibrillin-1 in human corneas with bullous keratopathy. *Cornea* 1998;17:309-14.
- 7 Takács L, Csutak A, Balázs E, et al. Immunohistochemical detection of  $\beta$ IG-H3 in scarring human cornea. *Graefes Arch Clin Exp Ophthalmol* 1999;237:529-34.
- 8 Skonier J, Neubauer M, Madisen L, et al. cDNA cloning and sequence analysis of  $\beta$ ig-h3, a novel gene induced in a human adenocarcinoma cell line after growth factor- $\beta$ . *DNA Cell Biol* 1992;11:511-22.
- 9 Munier FL, Korvatska E, Djemai A, et al. Keratoepithelin mutations in four 5q31-linked corneal dystrophies. *Nat Genet* 1997;15:247-52.
- 10 LeBaron RG, Bezverkov KI, Zimmer MP, et al.  $\beta$ ig-h3, a novel secretory protein inducible by transforming growth factor- $\beta$ , is present in normal skin and promotes the adhesion and spreading of dermal fibroblasts in vitro. *J Invest Dermatol* 1995;104:844-9.
- 11 Kublin CL, Cintron C.  $\beta$ ig-h3 is associated with normal development of extracellular matrices in human fetal eyes. [ARVO Abstract] *Invest Ophthalmol Vis Sci* 1996;37:S327.
- 12 Chiquet-Ehrismann R. What distinguishes tenascin from fibronectin? *FASEB* 1990;4:598-604.
- 13 Sage EH, Bornstein P. Extracellular proteins that modulate cell-matrix interactions: SPARC, tenascin, and thrombospondin. *J Biol Chem* 1991;266:14831-4.
- 14 Erickson HP. Tenascin C, tenascin R, and tenascin X: a family of talented proteins in search of functions. *Curr Opin Cell Biol* 1993;5:869-76.
- 15 Touri A, Uusitalo H, Thornell L, et al. The expression of tenascin-X in developing and adult rat and human. *Histochem J* 1999;31:245-52.
- 16 Chiquet-Ehrismann R, Hajios C, Matsumoto K. The tenascin gene family. *Perspect Devel Neurobiol* 1994;2:3.
- 17 Bristow J, Tee MK, Gitelman SE, et al. Tenascin-X: a novel extracellular matrix protein encoded by the human XB gene overlapping p450c21B. *J Cell Biol* 1993;122:265-78.
- 18 Carnemolla B, Laepriani A, Borsi L, et al. Human tenascin-R complete primary structure, pre-mRNA alternative splicing and gene localization on chromosome 1q23-q24. *J Biol Chem* 1996;271:8157-60.
- 19 Rocchi M, Archidiacono N, Romeo G, et al. Assignment of the gene for human tenascin to the region q32-q34 of chromosome 9. *Hum Genet* 1991;86:612-22.
- 20 Gulcher JR, Alexakos MJ, Le-Beau MM, et al. Chromosomal localisation of the human hexabranchion (tenascin) gene and evidence for recent reduplication within the gene. *Genomics* 1990;6:616-22.
- 21 Jones FS, Hoffman S, Cunningham BA, et al. A detailed structural model of cytotactin: protein homologies, alternative RNA splicing, and binding regions. *Proc Natl Acad Sci USA* 1989;86:1905-9.
- 22 Chiquet-Ehrismann R, Matsuoka Y, Hofer U, et al. Tenascin variants: differential binding to fibronectin and distinct distribution in cell cultures and tissues. *Cell Reg* 1991;2:927-38.
- 23 Kaplony YL, Zimmermann DR, Fischer RW, et al. Tenascin Mr 220,000 isoform expression correlates with corneal migration. *Development* 1991;112:605-14.
- 24 Tuori AJ, Virtanen I, Aine E, et al. The expression of tenascin and fibronectin in keratoconus, scarred and normal human cornea. *Graefes Arch Clin Exp Ophthalmol* 1997;235:675-82.
- 25 Maseruka H, Bonshek RE, Tullo AB. Tenascin-C expression in normal, inflamed and scarred human corneas. *Br J Ophthalmol* 1997;81:677-82.
- 26 Bonshek RE, Ridgway AEA, Tullo AB, et al. The time course and patterns of expression of tenascin-C (TN-C) variants in human corneal wound healing [ARVO Abstract]. *Invest Ophthalmol Vis Sci* 1999;40:S36 (Abstract no 1780).
- 27 Maseruka H, Ridgway A, Tullo A, et al. Developmental changes in patterns of expression of tenascin-C variants in the human cornea. *Invest Ophthalmol Vis Sci* 2000;41:4101-7.
- 28 Zaidi TS, Hassan A, Panjwani N. Localization of fibrillin in normal human and bovine corneas. [ARVO Abstract] *Invest Ophthalmol Vis Sci* 1991;32:S875.
- 29 Wheatley HM, Traboulsi EI, Flowers BE, et al. Immunohistochemical localization of fibrillin in human ocular tissue. *Arch Ophthalmol* 1995;113:103-9.
- 30 Sakai LY, Keene DR, Engvall E. Fibrillin, a new 350-kD glycoprotein, is a component of extracellular microfibrils. *J Cell Biol* 1986;103:2499-509.
- 31 Quantock AJ, Meek KM. Proteoglycan distribution in the corneas of individuals with bullous keratopathy. *Biochem Soc Trans* 1990;18:958.

- 32 Eagle RC, Laibson PR, Arentsen JJ. Epithelial abnormalities in chronic corneal edema: A histopathological study. *Trans Am Ophthalmol Soc* 1990;87:107-24.
- 33 Mohan RR, Liag QW, Kim WJ, et al. Apoptosis in the cornea: further characterisation of Fas/Fas ligand system. *Exp Eye Res* 1997;65:575-89.
- 34 Streeten BW, Klintworth GK, Egle RC, et al. Immunolocalization of  $\beta$ ig-h3 protein in 5q31-linked corneal dystrophies and normal corneas. *Arch Ophthalmol* 1999;117:67-75.
- 35 Gibson MA, Hatzinikolas G, Kumaratilake JS, et al. Further characterization of proteins associated with elastic fiber microfibrils including the molecular cloning of MAGP-2 (MP 25). *J Biol Chem* 1996;271:1096-1103.
- 36 Hashimoto K, Noshiro M, Ohno S, et al. Characterization of a cartilage-derived 66kDa protein (RGD-CAP/ $\beta$ ig-h3) that binds to collagen. *Biochim Biophys Acta* 1997;1355:303-14.
- 37 El-Shabrawi Y, Kublin CL, Cintron C. mRNA levels of  $\alpha$ 1(VI) collagen,  $\alpha$ 1(XII) collagen and  $\beta$ ig in rabbit cornea during normal development and healing. *Invest Ophthalmol Vis Sci* 1998;39:36-44.
- 38 Cintron C, Burrows R.  $\beta$ ig is bound to type IV collagen in corneal stroma. [ARVO Abstracts] *Invest Ophthalmol Vis Sci* 1997;38:S682.
- 39 Escribano J, Hernando N, Ghosh S, et al. cDNA from human ocular ciliary epithelium homologous to beta ig-h3 is preferentially expressed as an extracellular protein in the corneal epithelium. *J Cell Physiol* 1994;160:511-21.
- 40 Hirano K, Klintworth GK, Zhan Q, et al.  $\beta$ ig-h3 is synthesised by corneal epithelium and perhaps endothelium in Fuchs' dystrophy corneas. *Curr Eye Res* 1994;15:965-72.
- 41 Maurice DM. The cornea and sclera. In: *The eye*. 1969;Vol 1:489-600.
- 42 Rosenbaum JT, Plank SR, Haung X-N, et al. Detection of the mRNA for the cytokines, interleukin-1 alpha and interleukin-8, in corneas from patients with pseudophakic bullous keratopathy. *Invest Ophthalmol Vis Sci* 1995;36:2151-6.
- 43 Tucker RP, Hammarback JA, Jenrath DA, et al. Tenascin expression in mouse: in situ localisation and induction in vitro by bFGF. *J Cell Sci* 1993;104:69-76.
- 44 Sakai T, Kawakatsu H, Ohta M, et al. Tenascin induction in tenascin non-producing carcinoma cell line in vivo and by TGF-beta 1 in vitro. *J Cell Physiol* 1994;159:561-72.
- 45 LaFleur DW, Fagin JA, Forrester JS, et al. Cloning and characterisation of alternatively spliced isoforms of rat tenascin. *J Biol Chem* 1994;269:20757-63.
- 46 Wood A, Couchman JR. Focal adhesions and cell matrix interactions. *Collagen Relat Res* 1988;8:155-82.
- 47 Mackie EJ. Tenascin is connective tissue development and pathogenesis. *Perspect Dev Neurobiol* 1994;2:125-32.
- 48 Borsi L, Allemani G, Gaggero B, et al. Extracellular pH controls pre-mRNA alternative splicing of tenascin-C in normal, but not in malignantly transformed cells. *Int Cancer* 1996;66:632-5.
- 49 Maguen E, Alba SA, Burgesson RE, et al. Alteration in corneal extracellular matrix following multiple refractive procedures: clinical and immunohistochemical study. *Cornea* 1997;16:675-82.
- 50 Azar DT, Gibson IK. Immunolocalization of fibrillin and type VII collagen in keratoconus corneas. [ARVO Abstract] *Invest Ophthalmol Vis Sci* 1990;31:S100.
- 51 Wreth VP, Williams KJ, Fisher EA, et al. UVB irradiation alters cellular responses to cytokines: role in extracellular matrix expression. *J Invest Dermatol* 1997;108:290-4.